2016

Similarity Measurement of Breast Cancer Mammographic Images Using Combination of Mesh Distance Fourier Transform and Global Features

Ravi Kasaudhan
South Dakota State University

SIMILARITY MEASUREMENT OF BREAST CANCER MAMMOGRAPHIC IMAGES USING COMBINATION OF MESH DISTANCE FOURIER TRANSFROM AND GLOBAL FEATURES

BY

RAVI KASAUDHAN

A thesis submitted in partial fulfillment of the requirements for the

Master of Science

Major in Computer Science

South Dakota State University

2016

SIMILARITY MEASUREMENT OF BREAST CANCER MAMMOGRAPHIC IMAGES USING COMBINATION OF MESH DISTANCE FOURIER TRANSFROM AND GLOBAL FEATURES

This thesis is approved as a creditable and independent investigation by a candidate for the Master of Science in Computer Science degree and is acceptable for meeting the thesis requirements for this degree. Acceptance of this thesis does not imply that the conclusions reached by the candidates are necessarily the conclusions of the major department.

Sung Y. Shin, Ph.D.
Thesis Advisor Date

Steven Hietpas, Ph.D.
Head, Electrical Engineering and Computer Science Department Date

Dean, Graduate School Date

TABLE OF CONTENTS

LIST OF FIGURES

LIST OF TABLES

ABBREVIATIONS

CADe	Computer-Aided Detection
CADx	Computer-Aided Diagnosis
CBIR	Content-Based Image Retrieval
CT	Computed Tomography
EMDFD	Enhanced Mesh Distance Fourier Descriptor
FD	Fourier Descriptor
MDFD	Mesh Distance Fourier Descriptor
MRI	Magnetic Resonance Imaging
MT	Microwave Tomography
ROI	Region of Interest
SVM	Support Vector Machine
WD	Wavelet Descriptor

ABSTRACT

SIMILARITY MEASUREMENT OF BREAST CANCER MAMMOGRAPHIC IMAGES USING COMBINATION OF MESH DISTANCE FOURIER TRANSFROM AND GLOBAL FEATURES

RAVI KASAUDHAN

2016

Similarity measurement in breast cancer is an important aspect of determining the vulnerability of detected masses based on the previous cases. It is used to retrieve the most similar image for a given mammographic query image from a collection of previously archived images. By analyzing these results, doctors and radiologists can more accurately diagnose early-stage breast cancer and determine the best treatment. The direct result is better prognoses for breast cancer patients.

Similarity measurement in images has always been a challenging task in the field of pattern recognition. A widely-adopted strategy in Content-Based Image Retrieval (CBIR) is comparison of local shape-based features of images. Contours summarize the orientations and sizes images, allowing for heuristic approach in measuring similarity between images. Similarly, global features of an image have the ability to generalize the entire object with a single vector which is also an important aspect of CBIR.

The main objective of this paper is to enhance the similarity measurement between query images and database images so that the best match is chosen from the database for a particular query image, thus decreasing the chance of false positives. In this paper, a method has been proposed which compares both local and global features of

images to determine their similarity. Three image filters are applied to make this comparison. First, we filter using the mesh distance Fourier descriptor (MDFD), which is based on the calculation of local features of the mammographic image. After this filter is applied, we retrieve the five most similar images from the database. Two additional filters are applied to the resulting image set to determine the best match. Experiments show that this proposed method overcomes shortcomings of existing methods, increasing accuracy of matches from 68% to 88%.

1. INTRODUCTION

Cancers figure among the leading causes of morbidity and mortality worldwide, with approximately 14 million new cases and 8.2 million cancer deaths in 2012 [1]. The number of new cases is expected to rise by about 70% over the next two decades.

According to the American Cancer Society, breast cancer is the second leading cause of death in women after lung cancer. It is estimated that breast cancer in females alone could lead to 15% of the total deaths in the U.S. for the year 2015. An estimated 231,840 new cases of invasive breast cancer are expected to be diagnosed among women in the U.S. during 2015; about 2,350 new cases are expected in men [2].

Breast abnormalities are defined by a wide range of features and may be easily missed or misinterpreted by radiologists while reading large quantities of mammographic images provided in screening programs. To help radiologists provide accurate diagnoses, a computer-aided detection (CADe) and computer-aided diagnosis (CADx) algorithm are being developed [3]. Diagnosing breast cancer at early stage leads to more effective treatment in patients, potentially saving lives.

The malignancy of breast cancer can be analyzed by comparing it with cases that previously occurred. Similarity analysis of images is a crucial step in this process. There are many screening techniques already developed in order to obtain visual images of breast cancer; these include: mammography, magnetic image resonance (MRI), computed tomography (CT), and microwave tomography (MT). Microwave Tomography (MT) [4, 5].

Screening mammography is currently the best available radiological technique for early detection of breast cancer [6]. Screening mammography enables detection of early signs of breast cancer such as masses, calcifications, architectural distortion and bilateral asymmetry. Many technological improvements have been made in mammography since its initial introduction. Digital mammography is identical to traditional film-screen mammography except for the electronic detectors that capture and display X-ray signals on a computer rather than directly on film. This digital process provides the opportunity to adjust the contrast, brightness and magnification of the image without additional exposure [7]. Mammograms offer high quality images with minimal cost and health hazard.

Other existing methods such as MRI work well is some cases, but they can occasionally be too sensitive and pick up some regions that are not cancerous. MRI images are of high quality but are relatively expensive to obtain. The main disadvantages of CT include availability, speed and lack of operator independence. Another disadvantage of CT is the need for intravenous contrast enhancement, which exposes the patient to risk of an allergic reaction [8]. Radiologists' misinterpretation of the lesion can lead to a greater number of false positive cases; 65-90% of the biopsies of suspected cancer turn out to be benign [9].

Most image processing algorithms consists of same basic steps such as preprocessing, segmentation, feature extraction and classification/similarity measurements. In our work, images from mammograms was used to do the similarity measurement as it a widely used method with large database availability. With the development of digital screening methods, the importance of CAD system has increased.

As most images taken today are digital, many image processing tools are available. Detection and diagnosis of breast cancer is becoming a huge area of research, in part because of the availability of digital images.

There are recent advances in the field of medical imaging analysis where images from different screening techniques are being used together for the analysis of suspicious masses in the breast. In [10], the authors combined screening with ultrasound and mammography compared to mammography alone for the analysis of breast cancer and found that adding a single screening ultrasound to the mammogram yielded an additional 1.1 to 7.2 cancers per 1000 high-risk women. In [11], the authors analyzed similarity of fibro-glandular breast tissue content measured from MRI and mammographic images by a mathematical model. In [12], comparison between MRI and contrast enhanced spectral mammography based on sensitivity, specificity, positive and negative predictive values have been analyzed. In [13], research was done on identification of breast cancer using integrated information from mammogram and MRI. The project was initially primarily focused on the analysis of MT images of the breast for the classification and similarity measurement of the cancerous masses. This was because MT is an emerging biomedical imaging model with great potential for non-invasive assessment of functional and pathological conditions of soft tissues [14]. Also, MT is a new alternative technique to detect breast cancer using smart phone based electronic healthcare system, making it readily accessible to the population at large, unlike other techniques like MRI and mammography [15]. As we already have a huge database for MRI and mammograms, the concept of similarity measurement between cross-platform imaging techniques such as MRI, mammograms and MTI could increase the dimension of analysis of suspicious

regions in the breast and hence the similarity measurement. So, combining different screening techniques in the field of similarity measurement was brought into light. But, currently due to a lack of sufficient and reliable data in MTI, the idea shifted to enhance the similarity of the existing methodology based on mammograms and apply the same concept on MTI if sufficient and reliable data are available. Hence, in our work the similarity measurement was limited to mammograms only and combining it with MTI can be a part of future work.

During the last decade, significant progress has been made in both the theoretical and practical research aspects of shape-based image retrieval [16, 17, 18]. Contours of an image provide a heuristic approach for finding similarity of medical images. In many applications, the internal content of the shape is not as important as the boundary. For example, in classification of the ROI of mammograms into malignant and benign, shape plays an important role. Hence, similarity measurement was chosen to retrieve the most similar image from the database which has already been classified as benign or malignant. Boundary-based techniques tend to be more efficient for handling shapes that are describable by their object contours [19]. Compared to color or texture, shape alone can represent the whole object but common shape features require hundreds of parameters to be represented explicitly [20]. So, important features within a shape can be extracted in a concise way so that similarity between images can be done efficiently without having any delay in computation and without compromise in reliability. The increasing interest in using shape features of objects for CBIR is not surprising, since shape is a more intrinsic property of objects than color and texture, and given the

considerable evidence that natural objects are recognized primarily based on their shape [21, 22].

There are mainly two approaches for shape-based image retrieval, namely, contour-based (boundary-based) and region-based. Region-based techniques often use moment descriptors to describe shapes. These descriptors include geometrical moments [23, 24], Zernike moments (ZM) [25, 26] and Legendre moments [25]. Although region-based approaches are global in nature and can be applied to generic shapes, they often involve intensive computation and fail to distinguish between objects that are similar [19]. In many applications, the internal content of the shape is not as important as its boundary. Boundary-based techniques tend to be more efficient for handling shapes that are described by their contours. There are many existing boundary-based techniques such as Fourier descriptors [27, 28, 29], curvature scale space [30, 31, 32], wavelet descriptors [33, 34], contour displacement [35], chain codes [36] and multi-resolution polygonal shape descriptors [37]. Fourier descriptors have been proven to be better than other boundary-based techniques in many applications [27-29, 38, 39]. Fourier descriptors not only overcome the weak discrimination ability of moment descriptors, but also overcome the noise sensitivity in shape signature representation. Other advantages of Fourier descriptors include easy normalization and preservation of information [40]. Shape signatures, which constitute an essential component of Fourier descriptors, reduce 2-D shapes to 1-D functions and hence facilitate the process of deriving invariant shape features using the Fourier transform. Also, the rotation, translation and scale invariance of images can be easily achieved using Fourier transforms; these are important consideration in image similarity.

In this work, a shape-based feature named the “mesh distance measure” was used for similarity measurement; this considers the relationship of each of the boundary points with all other points in 2-D space. This method finds the shape feature such that even minor changes in the image contours could be traced and hence generate optimum results. This is used in the first filter in the process of similarity measurement: mesh distance Fourier descriptors (MDFD). In total, three levels of filters were implemented for the selection of a similar image to the query image.

In an image, we can have both local and global features and each type has its own advantages in similarity measurement. Global features have the ability to generalize an entire object with a single vector. Local features, on the other hand, are computed at multiple points in the image and are resistant to clutter and occlusion [41]. As global features together with local features add more information to an image than local features alone, the similarity measure of MDFD was enhanced by adding these global features: area ratio between the region of interest (ROI) and its minimum bounding rectangle, convexity, eccentricity and solidity. The second and third level of filters for filtering out similar images consists of these global features. In [41], the authors combined local and global features and used them for object recognition and found that doing so, there was a reduction of over 20% in the error rate. The idea of combining global and local features by [42] proved to be more effective in image retrieval and resulted in improved accuracy. As mentioned in [43], an image can be described either by its local features — which are associated with the contours of the shape — or by global features that describe the region of the shape. By combining the two, results revealed that the proposed method outperforms the existing method of image retrieval. Hence, in this paper MDFD was

combined with consideration of global features to enhance the performance of the system. The resulting algorithm is named Enhanced Mesh Distance Fourier Descriptor (EMDFD).

This paper binary images of the ROI of actual mammograms, which were classified into single objects using known classification methods such as K-means and the SVM algorithm, were used. Binary images were considered because in this work, we are dealing with contours and some global that can be extracted from binary images. Moreover, working with binary images reduces the processing time as the system does not have to deal with many intensity levels.

The organization of the rest of this paper is as follows. Section 2 describes global features and contour-based local features currently used in the area of similarity measurement. Section 3 briefly describes Fourier transforms and Fourier descriptors. Section 4 describes the existing method that we compare our proposed method against. Section 5 describes the proposed method in detail. Section 6 contains experimental results and conclusions drawn from the work.

2. LITERATURE REVIEW

2.1 Basic Overview

A feature is defined as a function of one or more measurements, each of which specifies some quantifiable property of an object, and is computed such that it quantifies some significant characteristics of the object [44]. Feature extraction is concerned with quantification of texture characteristics in terms of a collection of descriptors or qualitative feature measurements, often referred to as feature vectors [45].

Most image processing algorithms include some common steps as shown in Figure 1. Other steps are added according to the nature and need for the specific project. The first step is preprocessing of the digitized images to reduce noise and improve quality of the image. It also helps in representing the image in a format which can be easily used for feature extraction. It involves smoothing of the image so that the contour of image closely represents the actual object represented by the digital image. The next step is feature extraction which is obtaining unique properties of an image in order to represent the image in terms of vector elements. This step is very important because all the information about an image is obtained in this step. The final step is classification/similarity measurement. In this work, similarity measurement of the image is performed based on the features extracted.

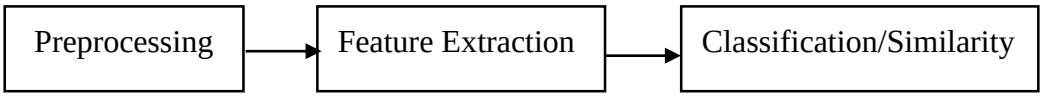

Figure 1: Common Steps for Image Processing Algorithms

2.2 Image Features

Image features can be broadly classified into two categories: general features and domain-specific features. General features are application-independent features such as color, texture and shape. General features can be further divided into pixel-level features, local features and global features. Domain-specific features are dependent on the application. For example, human faces and fingerprints could be considered domain-specific features.

2.2.1 Color

Color is a visual feature widely used in the process of image retrieval. In many cases, color plays an important role in pointing out differences between images. Each pixel in an image has an associated color consisting of red (R), green (G), blue (B) components of varying intensity. Each RGB combination can be reduced to a single grayscale value with an intensity ranging from 0 to 255, which can then be further reduced to a binary value of 0 or 255. Image consisting of RGB color pixels have many advantages like robustness, effectiveness, implementation simplicity, computation simplicity. Color features are used in a variety of image comparison considerations like color histogram, moment based color distribution features, color correleogram and color coherence vector. However, in some cases, color does not provide enough information that can be used for image retrieval. For example, in mammograms we have grayscale images and feature extraction done on the basis of RGB intensity levels may cause erroneous results.

2.2.2 Texture

Texture is a useful feature relevant to a wide range of images. It is generally believed that human visual systems use texture for recognition and interpretation. In general, color is usually a pixel-specific property, while a texture is a measure for group of pixels [46]. As such, texture is one of the most important features used to classify and recognize objects and has been used in finding similarities between images in multimedia databases. However, texture on its own does not provide enough information for finding similar images, but it can be used to classify textured images from non-textured ones and then be combined with another visual attribute like color to make the retrieval more effective [44]. Texture features can be broadly classified into spatial texture features and spectral texture features. Spatial texture features are extracted from the pixel-wise computation of an image while in spectral texture features, images are transformed into frequency domain.

2.2.3 Shape

Shape is known as important cue for human beings to identify and recognize real-world objects. Computationally, shapes are encoded as simple geometric forms such as straight lines in different directions [46]. Shape-based image retrieval is performed by measuring the similarity between shape features [44]. A shape descriptor, also known as a shape signature, is a set of numbers produced to describe a given shape feature. A descriptor aims to quantify shape in ways that agree with human intuitions [47]. Some examples of shape signatures include radial distance, chord-length distance, angular functions, triangular centroid area, triangular area representation, complex coordinates, polar coordinates and angular radial coordinates. Shape-based features can be broadly

classified in two types namely contour-based features and region-based feature. In region-based features, the pixels within a shape are used to obtain shape representation. Region-based features are commonly described by moment descriptors. To determine the contour-based features, the information at the boundary of the image is taken into consideration.

In our paper, binary images were used, so extraction of contour-based features seemed to be more reasonable than region-based shape descriptors. Also, color features and texture features do not apply to binary images. By using contour-based features, the complexity of the methodology is reduced without affecting the representation of the image, unlike when using texture feature methods. Hence, the main focus will be on shape-based method for feature extraction. The detailed description of contour- and region-based shape features is discussed below.

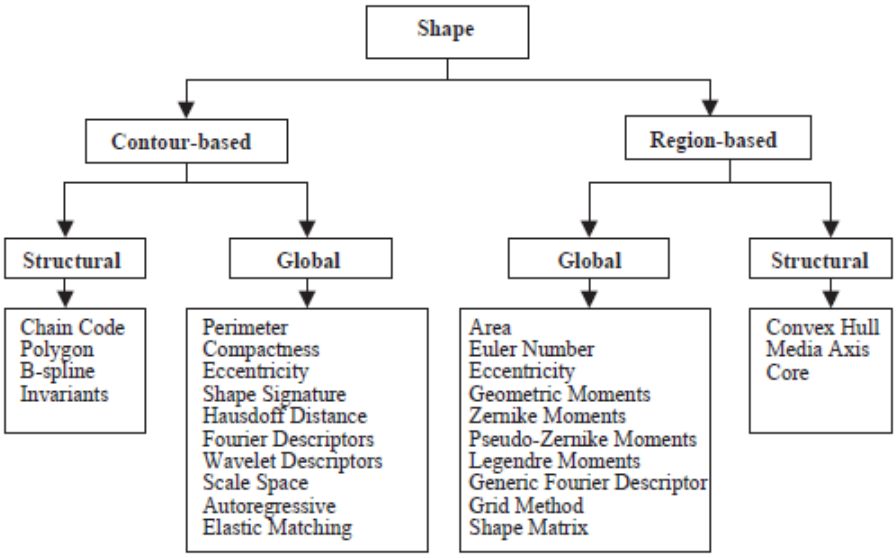

Figure 2: Different Shape-Based Features

2.2.3.1 Contour-Based

Contour-based techniques only exploit boundary information of a shape. Contour-based method can be divided into two types of shape modelling: structural (discrete approach) and global (continuous approach). Structural methods break the shape boundary into segments called primitives and the final representation is usually a string or a graph (or tree). Similarity measure is done by comparing the resulting strings or graphs. Continuous approaches do not divide shape into sub-parts; instead, usually a feature vector is derived from the integral boundary which is then used to describe the shape. The measure of shape similarity is usually a metric distance between the acquired feature vectors.

2.2.3.1.1 Structural Method

Using a structural approach, shapes are broken down into boundary segments called primitives. Structural methods differ in the selection of primitives and organization of the primitives for shape representation. Common methods of boundary decomposition are based on polygonal approximation, curvature decomposition and curve fitting [48]. The result is encoded in a string of general form:

$$S = s_1, s_2, \dots, s_n \tag{1}$$

where s_i may be an element of a chain code, a side of a polygon, a quadratic arc, a spline, etc. s_i may contain a number of attributes like length, average curvature, maximal curvature, bending energy and orientation.

2.2.3.1.2 Global Method

Global contour shape representation techniques usually compute a multi-dimensional numeric feature vector from the shape boundary information. The matching between shapes is a straightforward process, which is usually conducted by using a metric distance, such as Euclidean distance or city block distance. Some common examples include perimeter, compactness, convexity, eccentricity and solidity.

2.2.3.2 Region-Based

In region-based method, all pixels within a shape region are taken into account to obtain the shape representation (unlike contour-based methods which take into account only boundary points). Common region-based methods use moment descriptors. Other region based methods include grid method, shape matrix, convex hull and media axis. Global methods can also be divided into global and structural methods, depending on whether they separate shapes into subparts or not.

2.2.3.2.1 Global Method

Global methods treat a shape as a whole, the resulting representation is a numeric feature vector which can be used for shape description. Similarity between shapes is simply measured by the metric distance between their feature vectors. Some examples include geometric moment invariants, algebraic moment invariants, generic Fourier descriptors and grid-based methods.

2.2.3.2.2 Structural Method

Similar to contour structural methods, region-based structural methods decompose the shape region into parts which are then used for shape representation and description. Some examples of this method include convex hull and medial axis.

There are many works that have made contributions to shape-based image retrieval. In [49] the only shape signature used in image retrieval was a polar transform with the distance and angle of each contour point having a common center. The method was also tested for invariant operations like translation, rotation and scaling. In [50] various contour functions such as cross section, radius vector, parametric constants, complex, tangent angle and curvature were analyzed. These methods were compared with statistical features, moment invariants, Fourier descriptors (FD), wavelet descriptors (WD) and random descriptors. In [51,52], multiscale FDs through the complex wavelet transform involving the coefficients of WD in each scale was introduced which resulted in improved FDs and curvature scale space descriptors (CSSD). In [53], the authors described the shape with respect to statistical distribution of edge pixels. They measured the local features within each of the angular divisions. The feature vector was constructed using FDs. It was found that the features were invariant to scaling and rotation. In [54] Zhang et al. evaluated various shape signatures for 1-D FD-based on features like centroid distance, area, affinity, position, chord length and curvature. The authors in [55] have used short Fourier transform (SFT) to increase the capability of the Fourier-based techniques to capture local features. However, SFT is not suitable for image retrieval because the matching process using SFT is computationally more expensive than traditional FDs. Arbter et al. [56, 57] used a complex mathematical analysis and proposed

a set of normalized descriptors that are invariant under any affine transformations. Invariance to affine transforms allows considerable robustness in the case of rotating shapes in all three dimensions. Most of the Fourier-based techniques utilize the magnitude of Fourier transform and ignore the phase information in order to achieve rotation invariance as well as make the descriptors independent from the starting point. However, Bartolini et al. [58] described a technique in which the phase information is exploited. Mocanu et al. [59] presented various ways of boundary-based shape representations such as FDs, turning angle, centroid radii, distance histogram and centroid radii with turning angle methods. Guru et al [60] attempted to combine the contour and region information of the object during its representation and description such that it would remain invariant to translation, rotation and scaling. Conseil et al. [61] compared FD and HU moments and found that efficiency increases for FDs by exhibiting greater robustness to real objects.

In general, using Fourier descriptors is a promising boundary-based approach for shape-based image retrieval as FDs are based on well-known Fourier theory, making them easy to normalize and interpret. In addition, the computational efficiency and compactness of FDs allow them to be well suited for online image retrieval. To derive the FDs of an image, the 2-D image is converted to 1-D signature. Fourier descriptors derived from different signatures can have significantly different effects on the results of retrieval [62].

In this work, mesh distance method has been proposed and tested for similarity measurement, which uses the concept of Fourier transforms for similarity measurement.

3. FOURIER TRANSFORM

Fourier transform are an important image processing tool used to decompose an image into its sine and cosine components. The output of the transformation represents the image in the frequency domain. Fourier transforms for digital images is also known as discrete Fourier transform (DFT).

Consider the N contour points of an image component as a discrete function $x(u) = (x_1(n), x_1(n))$. Using this function we can define a discrete complex function $u(n)$ as,

$$u(n) = x_1(n) + jx_2(n) \tag{2}$$

$u(n)$ can be transformed into the frequency domain by DFT. The result can be transformed back into the spatial domain via the inverse discrete Fourier transform (IDFT) without any loss. DFT and IDFT are defined as $a(k)$ and $u(n)$, respectively.

$$a(k) = \frac{1}{N}\sum_{n=0}^{N-1} u(n)e^{-j2\pi kn/N} \quad k = -\frac{N}{2}, \dots, \frac{N}{2} - 1 \tag{3}$$

$$u(n) = \sum_{k=0}^{N-1} a(k)e^{j2\pi kn/N} \qquad n = -\frac{N}{2}, \dots, \frac{N}{2} - 1 \tag{4}$$

The coefficients $a(k)$ are also called Fourier descriptors [63]. They represent the discrete contour of a shape in the Fourier domain.

Certain geometric transformations of the contour function $u(n)$ can be related to simple operations in the Fourier domain. Translation by $u_0 \epsilon C$ affects only the first Fourier descriptor $a(0)$, while the other Fourier descriptors retain their values. Scaling of the contour with a factor α leads to scaling of the Fourier descriptors by α. Rotating the

contour by an angle θ_0 yields a constant phase shift of θ_0 in the Fourier descriptors. Changing the starting point of the contour by n_0 positions results in a linear phase shift of $2\pi n_0 k/N$ in the Fourier descriptors [63].

The contour functions are made invariant against translation by setting the first Fourier descriptor $a(0)$ to zero which moves the centroid of the contour onto 0. Since the contours are traced counterclockwise and describe a nonzero area, we can rely on the fact that the second Fourier descriptor $a(1) = r_1 e^{j\varphi}$ is nonzero [64] (tracing it clockwise would imply that $a(-1)$ is nonzero for a contour with nonzero area). Therefore, we can divide all Fourier descriptors by the magnitude of the second Fourier descriptors to obtain a scale-invariant vector: $a(k) = a(k)/a(1)$. Rotation invariance could be achieved by simply taking the magnitude of each Fourier coefficient.

With Fourier descriptors, global shape features are captured by the first few low frequency terms, while higher frequency terms capture finer features of the shape. Apparently, Fourier descriptors not only overcome the weak discrimination ability of moment descriptors but also overcome the noise sensitivity in the shape signature representations [65]. Recently, wavelet descriptors have also been used for shape representation [66, 67]. Wavelet descriptors have an advantage over Fourier descriptors in that they achieve localization of shape features in joint-space, i.e., in both spatial and frequency domains. However, the use of wavelet descriptors involve intensive computations in the matching stage as wavelet descriptors are not rotation-invariant.

4. EXISTING METHOD

Our proposed method is compared with an existing method named as sectorized object matching (SOM) for finding similarity in shapes developed in our lab [68]. The overall methodology of this method is shown in Figure 3.

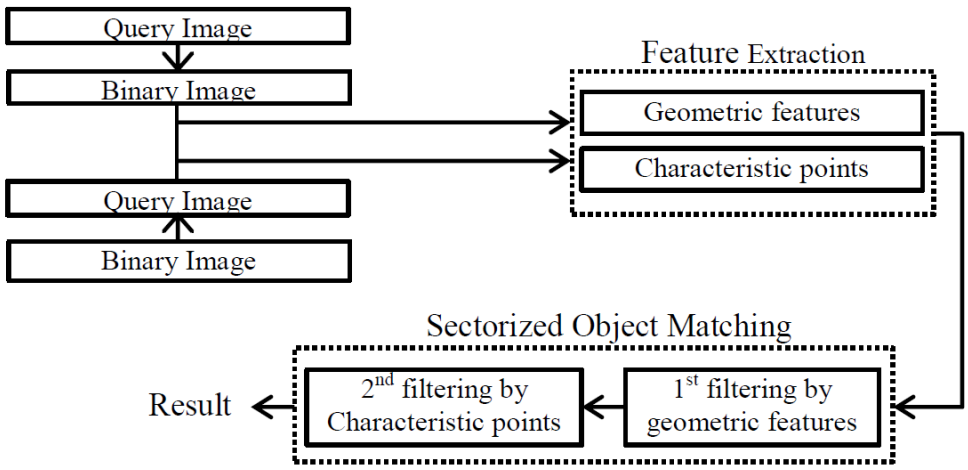

Figure 3: Diagram for Sectorized Object Matching

The figure shows that the method contains two different steps, namely feature extraction and sectorized object matching consisting of two levels of filtering.

4.1. Feature Extraction

The feature extraction consists of geometric features and characteristic points of the image to express shape representation of the image. Geometric features consist of calculation of center of gravity (or simply centroid) of image and area percentage, which is ratio of foreground pixels (white pixels) against minimum boundary rectangle of the object. Following equation shows the description of the area.

$$\frac{A_{white}}{A_{MBR}} \tag{5}$$

A_{white} is number of foreground pixels in the binary image. A_{MBR} is the minimum boundary rectangle that has the target object inside. By dividing the A_{white} by A_{MBR}, percentage of white mass in the rectangle was calculated, which was used as the source for first level filtering. The second level of filtering was based on the characteristic points obtained from the contours of the image. The goal was to retrieve the same number of characteristic points on every object images. By performing 360-degree clockwise scanning from the centroid of the object, the contour of the image was drawn and the image was divided into 8 equal sections based on equal angle. In each section, two characteristic points named Characteristic Point 1 (CP1) and Characteristic Point 2 (CP2) were extracted; thus, there were 16 characteristic points for each image.

Let C be the centroid of the object, S be the pixel point on the contour on the angle θ of the centroid. CP1 was obtained by comparing the minimum Euclidean distance from the centroid to the contour at every angle for each sector and CP2 was obtained by comparing the maximum distance.

$$CP1 = \min(d(C, S, \theta)) \tag{6}$$

$$CP2 = \max(d(C, S, \theta)) \tag{7}$$

For consistency, it was defined which CP would come first for each sector. SP1 represents first characteristic point which was found by comparing the angle θ of the CPs. Whichever CP (out of CP1 and CP2) with smallest angle was considered SP1; the CP with largest angle was considered SP2. It was obtained by equations (8) and (9).

$$SP1 = \min(CP1(\theta), CP2(\theta)) \tag{8}$$

$$SP2 = \max(CP1(\theta), CP2(\theta)) \tag{9}$$

4.2. Sectorized Object Matching

Sectorized object matching consisted of two filtering processes: geometric feature filtering and characteristic point matching.

The first filtering was based on the percentage area calculation. Equation (10) shows how k candidates were chosen from first filter.

$$GC[k] = \min(DF(Q_{Area}, \dots, D_{Area})) \tag{10}$$

where, Q_{Area} is the area of the query object and D_{Area} is area of the database images. GC represents the array of candidates to be chosen. DF is the absolute value of the difference between query image's area and area of the image from the database.

Characteristic point matching is done based on the k images retrieved from geometric feature filtering and query image. The average of sum of difference between the characteristic points of the query image and database images is calculated. The database image having the least value of the difference is considered as the most similar image to that query image.

The results obtained from this method are satisfactory but this method has many weak points that need to be considered.

Disadvantages:

1. The whole image is represented with only 16 characteristic points; this may result in critical information loss of the contour that makes the image unique.

2. The area ratio calculation for first-level filtering is based on the minimum bounding rectangle which is rotation-invariant. Hence, if the same image is rotated, the area ratio can come to be quite different, thus changing the result.
3. The method is scale-invariant, as well. It calculates similarity based on difference of the minimum and maximum distances from the centroid. If the same image is enlarged or compressed, the difference can vary a lot making it unsuitable to measure similarity of such images.
4. The method was tested with a variety of images and was found that it was not compatible with all sorts of images, thus limiting its application.
5. The method is very slow. It takes around 40-50 seconds to perform a single test.

5. PROPOSED METHOD

In this paper, a shape-based method named mesh distance Fourier descriptor (MDFD) was introduced, which exploits the concept of Fourier transforms to retrieve the most similar image from the database and is compared with Sectorized Object Matching (SOM) described in Section 4. The performance of MDFD was then enhanced by adding some geometric features and global features; this enhanced method is named the Enhanced Mesh Distance Fourier Descriptor (EMDFD). The proposed method consists of three filtering levels for retrieving the most similar image from the database. The first filter is based on the calculation of Euclidean distance of the Fourier descriptors of mesh distance which is present in MDFD. The second and third levels of filtering — which are based on the geometric and global features, respectively — are part of EMDFD. Both MDFD and EMDFD will be described separately in subsequent sections.

5.1. Mesh Distance Fourier Descriptor (MDFD)

Figure 4 shows the basic flowchart of the proposed method used for similarity measurement. The input image and database images are passed through different sections and important features are extracted which are then used for the similarity measurement using Euclidean distance.

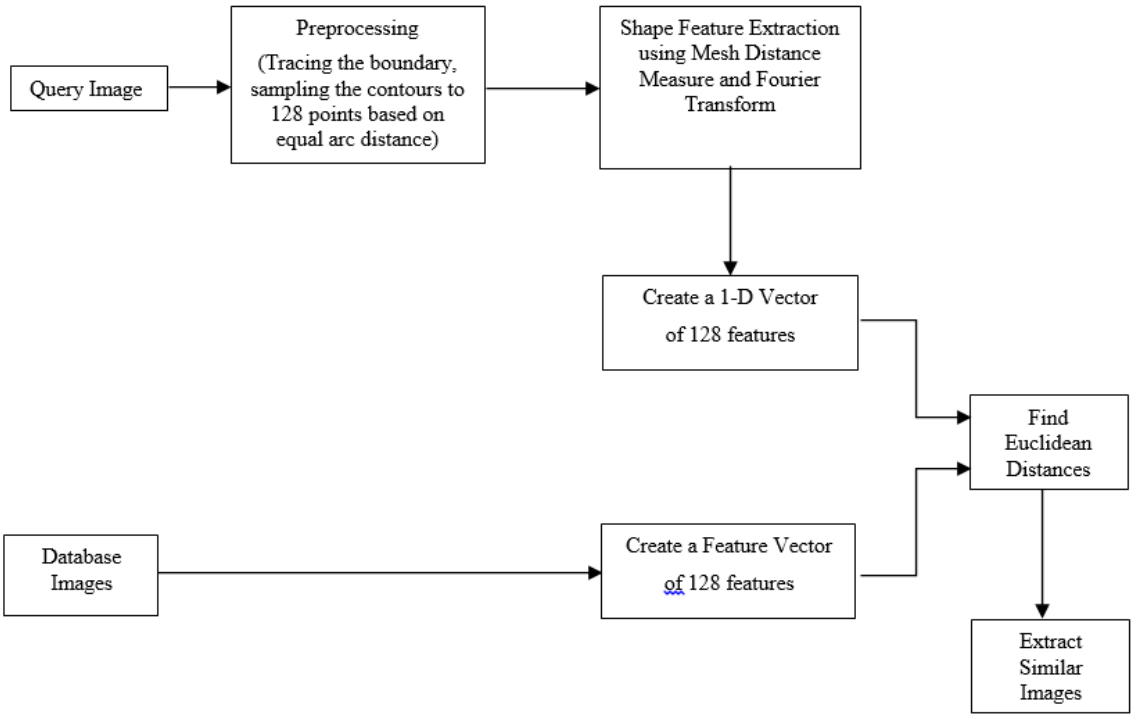

Figure 4: Flowchart for Similarity Measurement Using Proposed Method

Both query and database images are binary images extracted from real mammogram images which are classified into single objects using known classification methods such as K-means and SVM algorithms. The details of the input image are described in detail in Section 5.1.1. Each tumor case is unique in nature and each tumor image has distinctive features. To measure the correctness of the method while comparing with SOM, the database images that are used by this method are all created from query image by making small pixel-wise modifications. During creation of the database images, care was taken that the intensity of the images was not changed.

Each of the sections in Figure 4 are described in detailed in the following sections.

5.1.1.Input Image

The input images used in this method are binary images, so each pixel has the value of either 0 or 1. These input images are the result of the extraction of the Region of Interest (ROI) on the corresponding raw mammogram images. Transformation of a real mammogram image ROI to a binary image is shown in Figure 5.

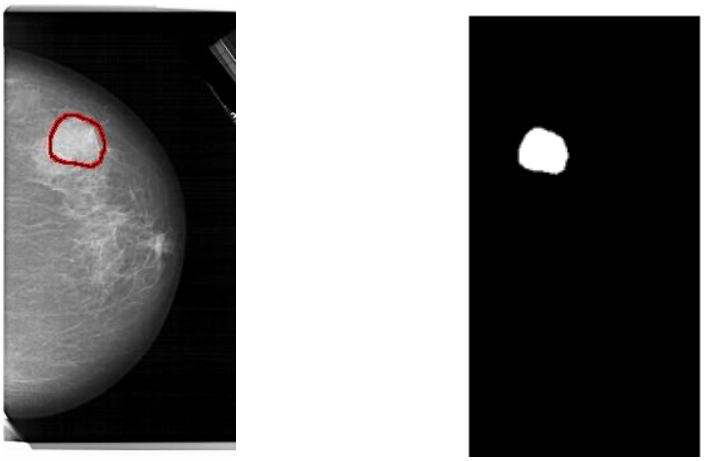

a) b)

Figure 5: a) Mammogram Image with ROI b) Binary Image of ROI

Figure 5a shows the actual mammogram image of a breast of a patient which contains a suspicious region to be analyzed with the ROI marked by doctors and radiologists. Figure 5b is the binary image for the ROI marked in 5a. All the images used in our method are obtained by this process.

Binary images were used because our method deals with the contour of the image and has nothing to do with the texture of the image. Binary images are sufficient to extract the contour of an image and also make the computation really fast, as we do not have to deal with the different intensity levels in the image.

Before the feature of the ROIs are extracted, the binary images are passed through preprocessing steps which standardizes all the images contours and perform smoothing of images to represent them to look similar to the actual image.

5.1.2.Database Images

Before any comparison was made, the original binary image was modified pixel-wise such that the images developed were quite similar and hence a good comparison could be made. In total, 25 binary images were modified such that each image had 3 similar images.

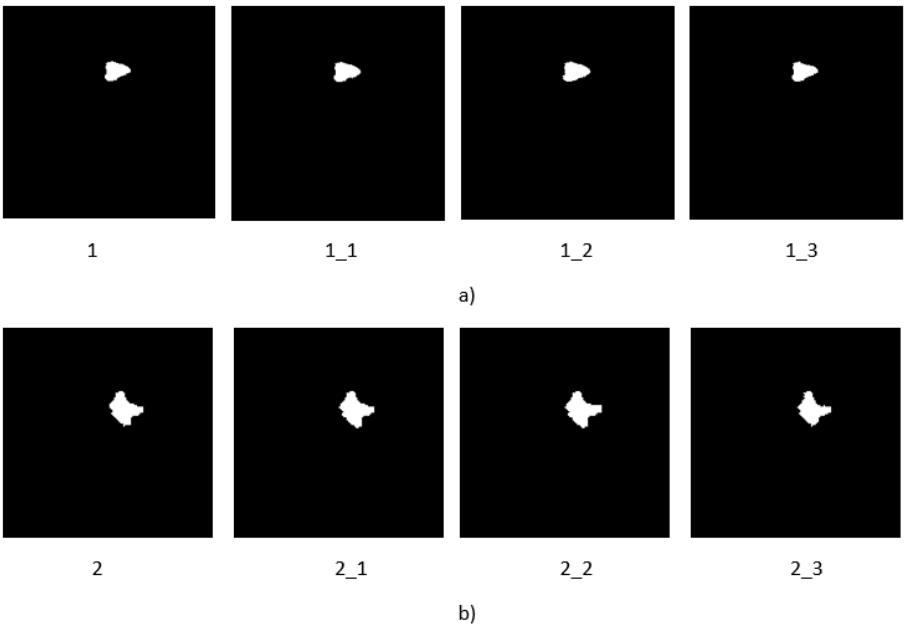

Figure 6: Binary Images with Modified Similar Images

In Figure 6, images 1 and 2 are the original images. Dissimilarity with the original images increases as we move towards the right because each image is modified from its previous images. In Figure 6b, image 2_3 is more dissimilar than image 2_2 and so forth. Both, the mesh distance method and SOM method selects only the most similar image

from the database. If image 1_1 is selected for image 1 then it is said to be matched, otherwise it is considered as mismatch.

As mentioned above, images 1_1, 1_2 and 1_3 in Figure 6 are the modified images corresponding to image 1. Image 1 is the actual ROI for the tumor; it is the image obtained from the mammogram in the form of a binary image. This was done because in the field, the tumor regions are so unique that to find a similar image is difficult. Hence, to evaluate the system, similar images were used to calculate the accuracy of the system. However, this method should also work for real-life cases, as well, even if there is not perfect similarity between images. So, in order to retrieve the most similar image using the images in the field, a certain value of Euclidean distance was used as a threshold to extract the most similar image. In our cases, a threshold value of 0.40 was used, which means that our method will retrieve images which have at least a 60% match with the query image. So, if the value of Euclidean distance falls within the given threshold, the image is considered to be similar to the query image.

5.1.3.Preprocessing Step

In the preprocessing step, the contours of the images are first traced in order to extract a closed 2-D boundary of the image. The image to be fed to the preprocessing step should be a binary image. After the contour points have been extracted, smoothing of contour is performed using spline interpolation in order to closely represent the contour of the original image. Before the shape features are extracted, 128 discrete boundary points are sampled based on equal arc distance; this is sufficient information to represent the original image. Figure 7 shows the results from the preprocessing step.

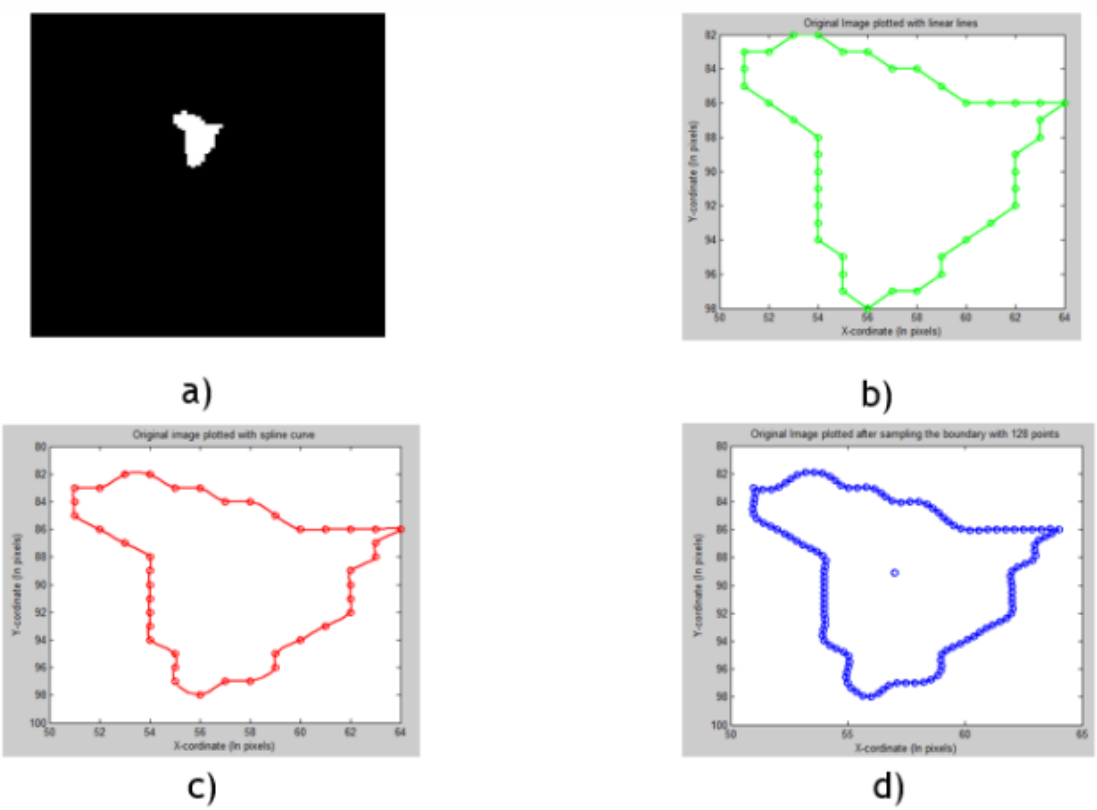

Figure 7: a) A Binary Image, b) Linearly-Traced Contour Image, c) Contour Smoothed using Spline Curve, d) Contour Re-sampled to 128 Points Based on Equal Arc Length

Also, during creation of the database images it was found that the image information which should contain in 2-D vector was changed to 3-D, creating unnecessary information in the image. Therefore, part of preprocessing involved converting the 3-D contents to a 2-D vector representation without losing any pertinent information from the image. After this conversion, further processing of the image was performed.

The image in 7b is the point when the boundary of the ROI is extracted and traced with linear lines. The boundary points representing the images are a bit random in nature. It can contain any number of points to represent the original image, which is not a good thing as images can be of any size and shape. So, this problem was noticed and resolved.

To solve this problem, each image was sampled to fixed number of boundary points. In this case, 128 boundary points were used to represent any image. Doing so, the comparison can be done properly and there is consistency in the method for all sorts of images. Sampling to 128 points was done on the basis of equal arc length on the boundary points such that the distance between each neighboring pixel is equal. Although there are other methods to sample a contour points like equal angle sampling, equal point sampling and equal arc length sampling, equal arc sampling was used because this method apparently achieves the best equal space effect, because the use of arc length as a signature parameter results in constant-speed traversal of the shape boundary [37]. Also, the smoothing of the contour points is done through spline interpolation so that the image contour looks like the original image.

5.1.4.Shape Feature Extraction

This is the most important aspect in the context of image similarity measurement. The feature should be significant enough to outperform the existing method mentioned in Section 4. After sampling the boundary of the image, the mesh distance is calculated. Mesh distance represents the sum of distances for each of the boundary points to all other points on the contour of the image. Hence, the name “mesh distance”.

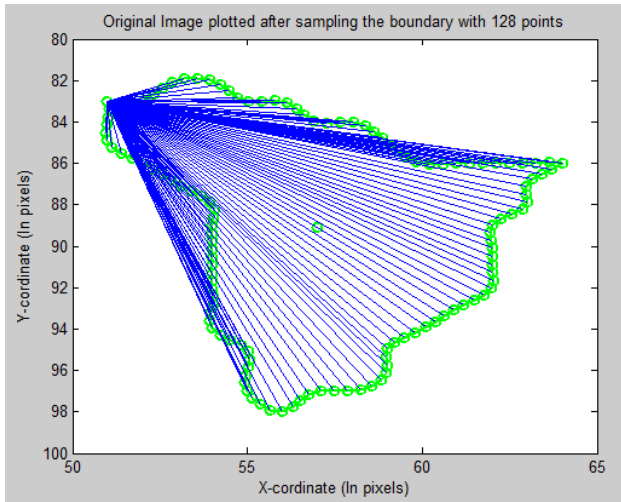

Figure 8: Mesh Distance Calculation for Boundary Points

Figure 3 shows a visual representation of mesh distance from one of the boundary points. To make the distance invariant to the translation, all the distances are calculated with respect to the centroid of the image [25].

Let the boundary points be represented by $I(x_k,y_k)$ where i = 1, 2, … , 128 and (x_c,y_c) be the centroid of the images. Then the mesh distance array can be calculated as,

$$Mesh\ Distance[i] = \sum_{k=1}^{128} \left(\sqrt{(x_c - x_i)^2 + (y_c - y_i)^2} + \sqrt{(x_c - x_k)^2 + (y_c - y_k)^2} \right) \qquad (11)$$

for i =1,2 …, 128

The mesh distance array is a 1* 128 matrix. Now the Fourier transform is calculated for the distance in the mesh array to find the Fourier descriptors which are used to describe the shape. Fourier descriptors are calculated by equation (12).

For a given image normalized to N points, the discrete Fourier transform of an arbitrary signature Z(u) is given by

$$a_n = \frac{1}{n}\sum_{u=0}^{N-1} Z(u)e^{-j2\pi nu/N} \tag{12}$$

where, n= 0,1, …, N-1

The coefficients a_n (n= 0,1, …, N-1) are called Fourier descriptors of the shape and are denoted by FD_n.

After calculating the FDs, only magnitude values are considered for the feature description. Also the values are normalized to a range of 0 to 1 so that all the images use have same frame of reference while being compared.

Several properties need to be considered after calculating the shape features. The features should be rotation-, scale- and starting-point-invariant. All these properties were tested and described in subsequent sections:

5.1.5.Rotation Invariance

Fourier transform coefficients contain information about both the magnitude and phase of the image. Taking only magnitude into consideration, we find the rotation-invariant property. Figures 4b and 4d represent the Fourier transform for the original image and the rotated image (rotated by 90° counterclockwise). So, we can say that the shape descriptor is rotation-invariant.

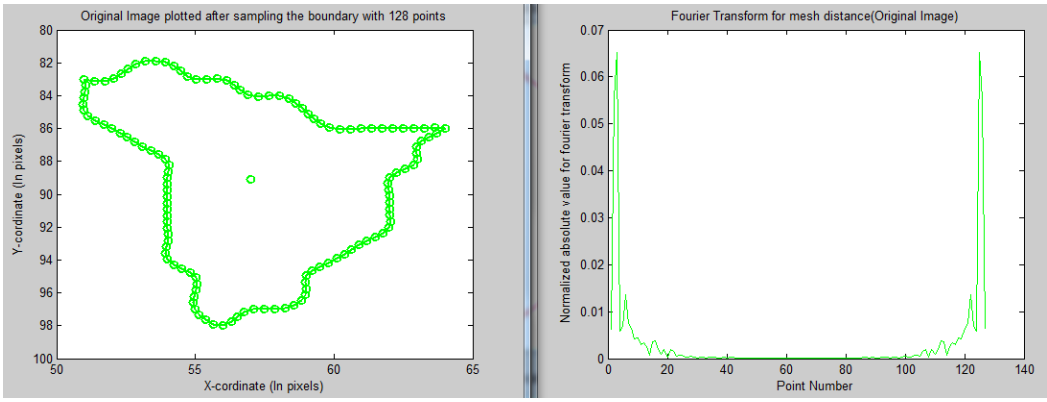

a) b)

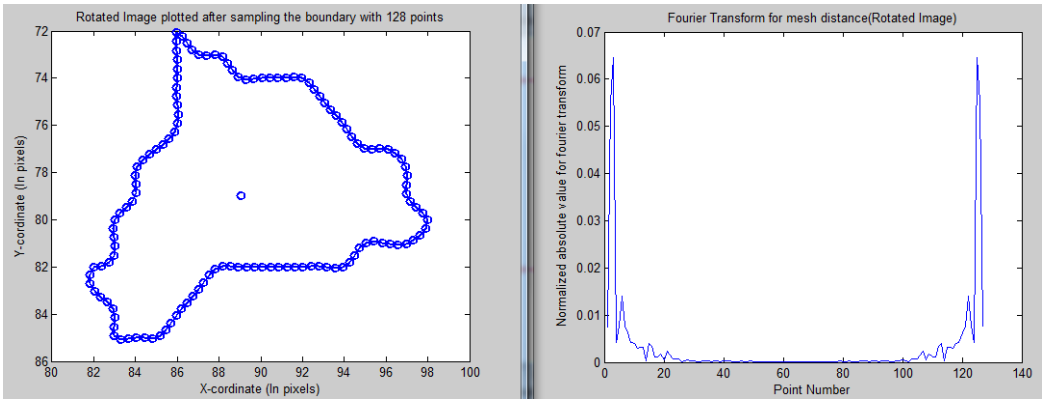

c) d)

Figure 9 : Rotation Invariance for Shape Descriptor a) Original Contour, b) Fourier Transform for Image ‘a’, c) Contour Obtained After Rotating Image by 90°, d) Fourier Transform of Rotated Image ‘c’.

5.1.6.Scale Invariance

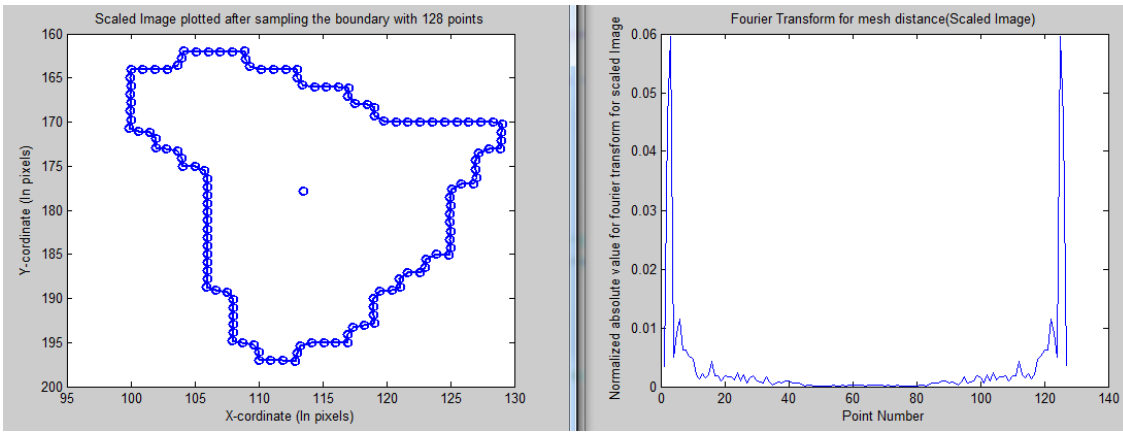

a) b)

Figure 10: a) Contour of Rescaled Image (scaled by factor 2); b) Fourier Transform of Scaled Image

The original image (Figure 9a) was scaled by a factor of 2 and the contour obtained is shown in the figure 5a. Figure 5b shows how the Fourier coefficients are similar to the original image. This demonstrates the scale invariance in our approach.

As the signature used for the shape description is real-valued, scale invariance of the FDs is achieved by dividing the magnitude of the first half descriptors by the non-frequency component (FD_0) [13].

$$F = \left[\frac{FD_1}{FD_0}, \frac{FD_2}{FD_0}, \dots, \frac{FD_{N/2}}{FD_0}\right]$$

5.1.7.Starting Point Invariance

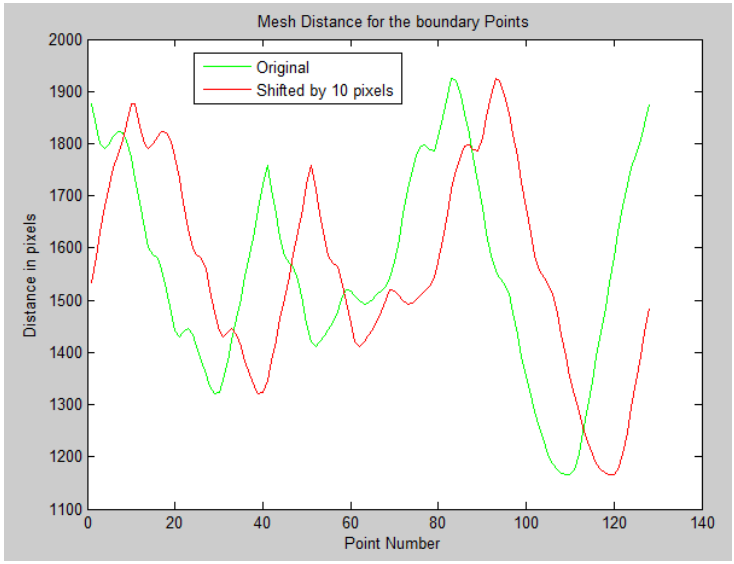

a)

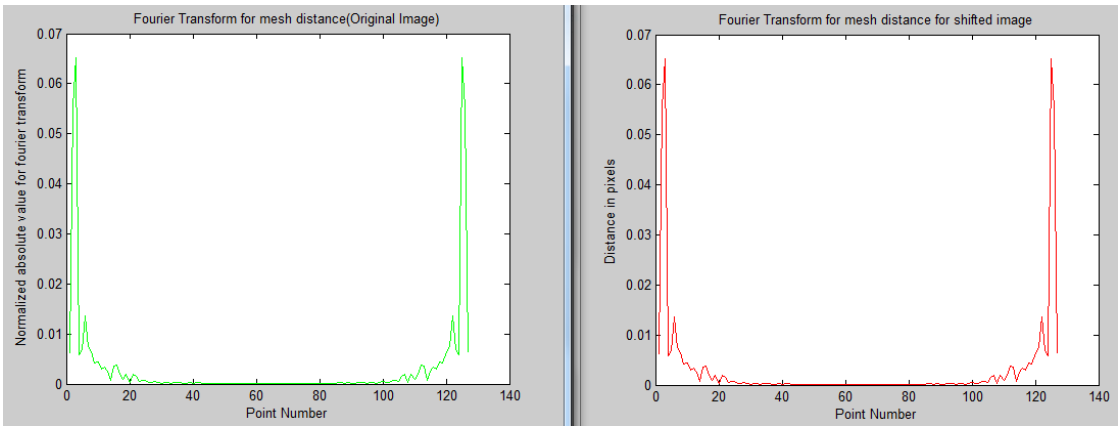

b) c)

Figure 11 : a) Mesh Distance vs. Point Number for Original Image (Green) and Image Shifted by 10 Pixels (Red), b) Fourier Transform of Original Image, c) Fourier Transform of Shifted Image

The robustness of the method was also tested through shifting the points of the image. Figure 11a shows the contours for the original (green) and shifted (red) image traced as a function of mesh distance. Figure 11a is representation of obtained feature (mesh distance) in a 2-D with boundary points on x-axis and mesh distance (in pixels) on

the y-axis. In order to ensure that our method yields results invariant to the starting point, different starting points on the image contour were chosen

In spite of the different starting points, the Fourier transform was found to be the same as shown in Figures 11b and 11c. Therefore, our method was starting-point-invariant.

Hence, from these test we can say that the proposed method is rotation-invariant, scale-invariant and starting-point-invariant. This proves to be important in determining image similarity.

5.1.8.Similarity Measurement

After Fourier descriptors for the query image and all the database images are stored in the vector, similarity measurement is performed based on Euclidean distance.

The similarity measure between two shapes indexed with M normalized Fourier descriptors is the Euclidean distance D between the normalized Fourier descriptors of the query image F^q and the normalized Fourier descriptors of an image from the database F^d [17].

$$D(P^d, P^d\ ) = \sqrt{\sum_{i=1}^{M} (f_i^q - f_i^d)^2} \tag{13}$$

where,

M = Number of Fourier descriptors (128 in this case)

D = Euclidean distance

F^q = Normalized Fourier descriptors of query image

F^d = Normalized Fourier descriptors of image from database.

Similarity between images is inversely proportional to D. Thus, if the Euclidean distance is 0, then there is a perfect match between the query image and database image.

5.2. Enhanced Mesh Distance Fourier Descriptor

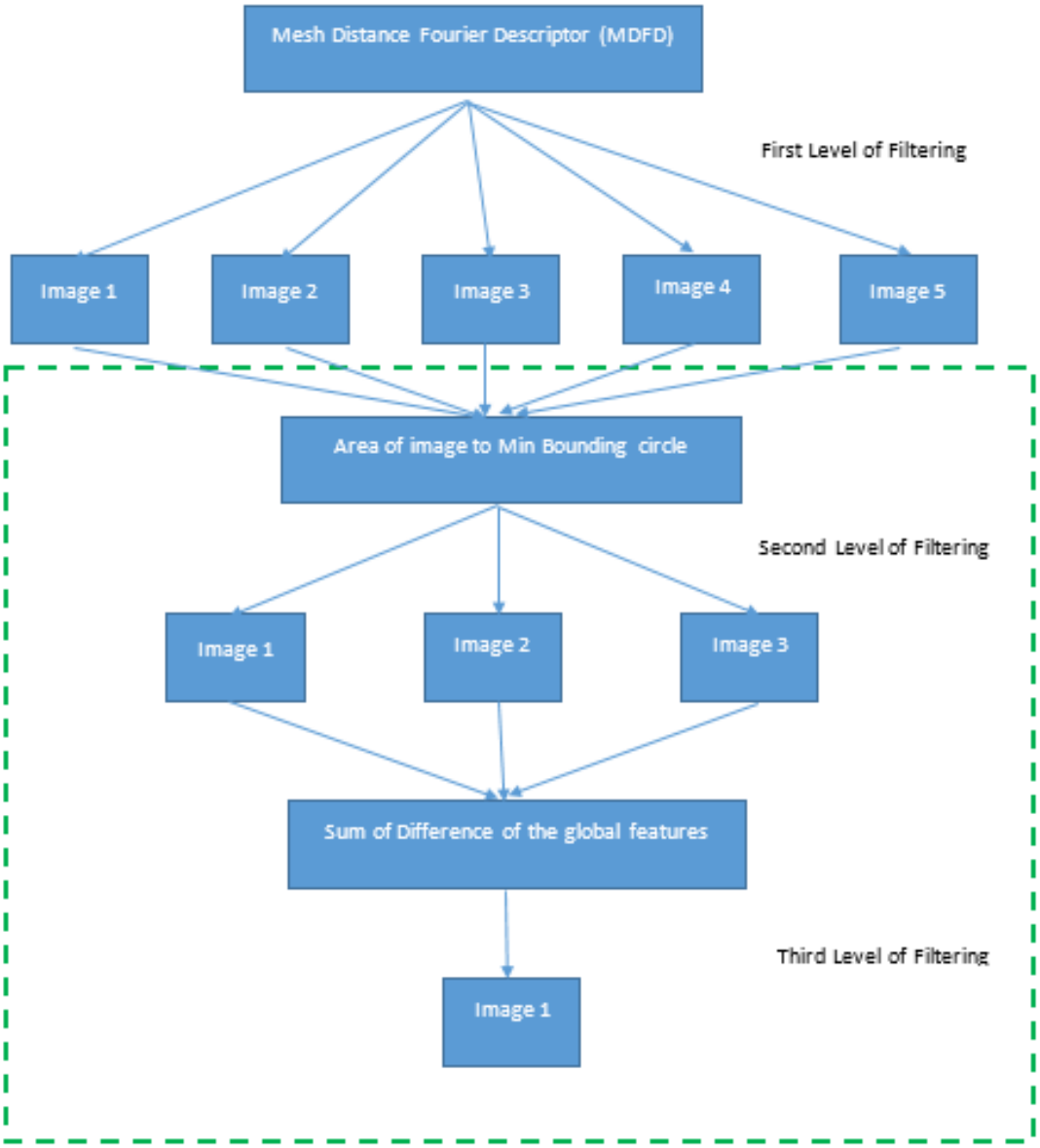

Figure 12 : Workflow of EMDFD with Extra Two Levels of Filtering Indicated in Dashed Box

The workflow of the EMDFD is shown in Figure 12 where two extra levels of filtering process have been added to the previous work (MDFD) to achieve higher accuracy in similarity measurement. MDFD extracts five similar images from the database using the first level of filtering as described in Section 5.1. EMDFD further processes these five images to refine the similarity measurement against the query image. The region in the dashed box in Figure 12 indicates those refinements. The details of the extra filtering steps are described in the following sections.

5.2.1.Second Level of Filtering

Here, area ratio is used to determine the three most similar images out of the five obtained from the first step. In this filter, the area of the ROI is divided by the area of the minimum bounding circle of the ROI. The area ratio is calculated by equation (14). This feature is calculated for all five images and the query image itself. The three images having the smallest absolute area ratio (also known as error ratio) with the query image are passed down through the filter for further processing. The error in area ratio is calculated by equation (15). If two or more images have same error ratio, the first image retrieved by MDFD is selected. For example, in Figure 15b if 2_17 and 3_16 have same error ratio, 2_17 gets higher priority over 3_16 for further processing.

Figure 13 shows tracing of the minimum bounding circle to the ROI. The white region is the ROI and the red circle is the minimum bounding circle. Thar ratio of these two areas is used in the second level of filtering.

$$Area\ Ratio = \frac{Area\ of\ the\ ROI}{Area\ of\ minimum\ Bounding\ Circle} \tag{14}$$

$$Error_{Area\ Ratio} = \left|Area\ Ratio_{Query\ Image} - Area\ Ratio_{Retireved\ Image}\right| \tag{15}$$

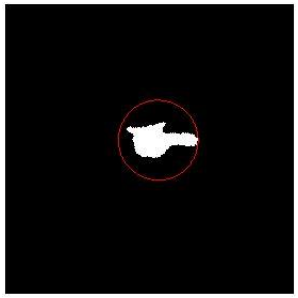

Figure 13: Minimum Bounding Circle of ROI

5.2.2.Third level of Filtering

The third level of filtering is based on global features; this helps to improve the accuracy obtained by MDFD, which is based only on local descriptors. The global features used are convexity, eccentricity and solidity.

The mathematical equations for each of these features are given below:

Convexity: ratio of perimeters of the convex hull, $O_{convexhull}$ over that of the original contour [22].

$$Convexity = \frac{O_{convexhull}}{O} \tag{16}$$

Eccentricity: length ratio between the major and minor axes of the minimum bounding rectangle [23]; also known as aspect ratio.

$$Eccentricity = \frac{Length\ of\ major\ axis}{Length\ of\ minor\ axis} \tag{17}$$

Solidity: the extent to which the shape is convex or concave, defined by

$$Solidity = \frac{A_s}{H} \tag{18}$$

where A_s is the area of the shape region and H is the convex hull area of the shape. The solidity of a convex shape is always 1 [46].

These features are calculated for the query image and the three most similar images output from the second filter. After these features are computed, average absolute difference between the query image and database images for the three features is calculated using equation (22). The image having the least error is selected as the most similar image compared to the query image. The error in convexity, eccentricity and solidity is calculated using equations (19), (20) and (21) respectively.

$$Convexity_{Error} = \left|Convexity_{QueryImage} - Convexity_{DBmage}\right| \tag{19}$$

$$Eccentricity_{Error} = \left|Eccentricity_{QueryImage} - Eccentricity_{DBmage}\right| \tag{20}$$

$$Solidity_{Error} = \left|Solidity_{QueryImage} - Solidity_{DBmage}\right| \tag{21}$$

$$Error_{GlobalFeatures} = \frac{Convexity_{Error} + Eccentricity_{Error} + Solidity_{Error}}{3} \tag{22}$$

5.2.3.Similarity Measurement

As this paper describes an enhanced MDFD method, the first level of filtering is done the same as MDFD, i.e., using Euclidean distance. This calculation is shown in equation (13)

```
Step 1 : Select the query image. (main.m)

Step 2 :
        For selected Image: (boundary_Sel.m)
            -Calculate a 1*128 feature vector using mesh Distance
             method
            -Caculate the global features (solidity, eccentricity
             and solidity)
            -Return the calculated values to main.m

Step 3 :
        For DatabaseImages (boundaryForAllImages.m)
            -Also calculate feature vectors for all the database images
            -Caculate the global features (solidity, eccentricity and
             solidity)
            -Return the caculated values for all the images to main.m

Step 4 :
        First Level of Filtering (main.m)
            -Calculate the euclidean distance between the feature
             vectors of query image and database images
            -make an array for the calculation of eculidean distance
              and sort the array with is ascending order
            -Extract the first five images based on the lowest five
             euclidean distance values and save in the separate folder

Step 5 :
        Second level of Filtering (boundingBox.m)
            -Calculate the area ratio for these five images
            -Find the error values for each of the images
            -Extract the lowest three values of the error.
            -If there two images same same error select the image based
             on the order obtained in First Level of filtering
            -Save the top three similar images in a separate folder

Step 6 :
        Third Level of Filtering (main.m)
            -Use the global features obtained from Step 1 and Step 2 to
             calculate absolute values of error
            -Take average of the three global features error
            -Select the image which has the lowest error.
            -Save final extracted image in a separate folder
```

Figure 14 : Algorithm for Whole Work

The second and third level of similarity measurement is done by calculating the error in the values of the query image and the retrieved similar images from the first level of filtering. The lower the error value, the more similar the image is with respect to query image.

In the second filtering process, $Error_{AreaRatio}$ is calculated for all five images extracted from first level using equation (15). The images having the smallest error values are selected for next level of filtering. From Table 1, it is clear that the images to be selected for the next level of filtering will be 1_18, 2_17 and 3_16.

In the third filtering process, $Error_{GlobalFeatures}$ is calculated using equation (22). It takes into consideration the average value for errors in convexity, eccentricity and solidity. It should be noted that the errors in the global features are the absolute values of the difference. The absolute values were taken into consideration because we were concerned only about the minimum difference value which could either be in the positive or negative range. So, taking absolute of the difference would achieve this goal and hence was applied.

6. EXPERIMENTAL RESULTS AND ANALYSIS

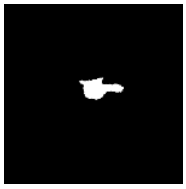

a)

b)

Figure 15: a) Query Image b) Top Five Similar Images Extracted by MDFD

Figure 15a shows a query image and Figure 15b shows the five most similar images retrieved from database using MDFD as described above. This figure uses a specific numbering system which will now be described. Taking for example image 1_18, the first number (1) indicates the order of similarity with the query image and the second number (18) is the index of the image in the database. So, in Figure 3, 1_18 is the most similar image and 5_50 is most dissimilar image according to MDFD. The images 1_18, 2_17 and 3_16 are the modified images as described in Section 5.1.2 in detail and 3_16 is the most similar image.

MDFD always picks the image with order of similarity equals 1. For the query image in Figure 15, it picks 1_18 as the most similar image. However, as mentioned in Section 5.1.2, images 3_16, 2_17 and 1_16 are the modifed images for the query image and 3_16 is the most similar one per the modification made.So, MDFD is picking the

wrong image. It should actually pick 3_16 as the most similar image. Hence, teo levels of filtering have been implemented to improve the performance of MDFD.

Table 1: Calculation of Error Based on Equation (15)

Image	Area of ROI	Area of Minimum Bounding Circle	Area Ratio	$Error_{Area\ Ratio}$
Query Image	1211	2178	0.56	-
1_18	1157	2015	0.57	0.01
2_17	1175	2046	0.57	0.01
3_16	1193	2112	0.56	0.00
4_51	425	741	0.57	0.02
5_50	461	780	0.59	0.03

Table 1 shows the error of area ratio for all the five retrieved images from MDFD. Among these five images, the three most similar images need to be chosen by the second filter.

At this point, 1_18, 2_17 and 3_16 are chosen for further processing because these three images have the smallest error ratio, as shown in Table 1. These images will be fed to the third filter for more refinement.

Table 2: Calculation of Error Based on Equation (11)

Image	Convexity	Eccentricity	Solidity	Error
Query Image	0.8358	0.8850	0.7631	-
1_18	0.8872	0.8922	0.7683	0.0179
2_17	0.8610	0.8948	0.7705	0.0142
3_16	0.8540	0.8884	0.7672	0.0085

In the third filtering level, the global features of convexity, eccentricity and solidity are calculated as well as their error values as described in Section 5.2.2 and tabulated in Table 2. From Table 2, we see that, 3_16 has the least error, so it is selected

as the most similar image. As expected EMDFD selected the right image as described above and in Section 5.1.2.

From this result, we can say that adding filters enhances the results and helps in retrieving the right image from the database.

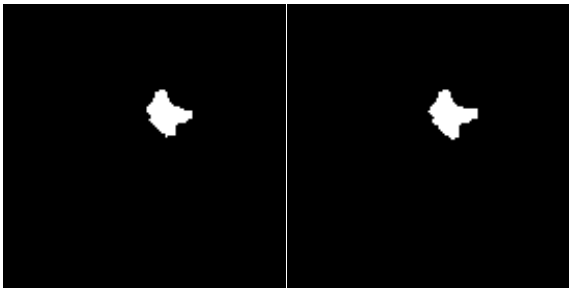

a) 2 b) 2_2

Figure 16: a) Original Image b) Similar Image Extracted from SOM

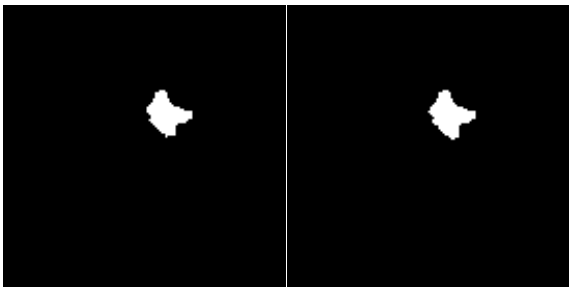

c) 2 d) 2_1

Figure 17: a) Original Image b) Similar Image Extracted from Proposed Method

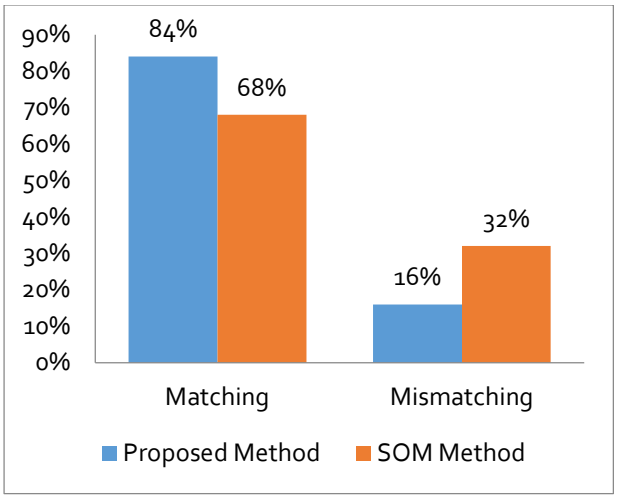

Figure 18: Similarity Results for Proposed Method and SOM

Figures 16 and 17 show the similar images extracted by SOM and the proposed method (MDFD), respectively. It is clear that SOM retrieved the wrong image while MDFD retrieved the correct one. Figure 18 shows the performance result for SOM and MDFD. A total of 25 images were fed to both SOM and MDFD and as seen in Figure 18, it is obvious that MDFD outperforms SOM by 16% in retrieving the most similar image from the database. The result shows that the proposed method provides a better similarity measurement than SOM method.

Also, MDFD was tested against a wide range of threshold values to see how the method responded in retrieving similar images from the database and how the performance changed.

Table 3: Similarity Measurements on Different Threshold Values

Threshold Value	Similarity Measurement %
0.9	84
0.8	84
0.7	84
0.6	84
0.5	84
0.4	84
0.3	76
0.2	40
0.1	12

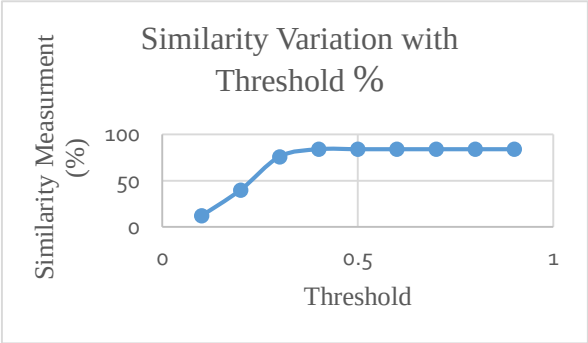

Figure 19 : Effect of Threshold on Similarity Measurement

Table 3 shows the percentage of similarity measurement using different threshold values. The graph in Figure 19 is as expected because if the threshold value is zero, the algorithm looks for a perfect match in the database, which is a rare case and hence no image is retrieved. As the threshold value is increased, the algorithm has a wider range to select a most similar match. The graph also indicates that a threshold value greater than 0.4 there is no improvement to the similarity measurement. This is because as the threshold value increases, images which are not that similar to the query image become candidates. However, as only the first image out of all the images is selected, there is no difference in the similarity percentage and the images are ordered according to the similarity to the query image.

a) 6 b) 6_3

Figure 20: a) Original Image b) Similar Image Extracted from MDFD

c) 6 d) 6_1

Figure 21: a) Original Image b) Similar Image Extracted from EMDFD

Figures 20 and 21 show the results obtained from MDFD and EMDFD. Here, image 6 has been fed to both the methods as the query image; the image extracted by each method is shown on the right of the query image. It is clear that adding filters to MDFD improved the accuracy of selection. The first method chose 6_3 (3_18 in Figure 3b) but the EMDFD chose 6_1 (3_16 in Figure 3b).

Both the methods were tested against 25 query images and it was found that the matching ratio was increased from 84% to 88% and the mismatching ratio was reduced from 16% to 12% as shown in Figure 22.

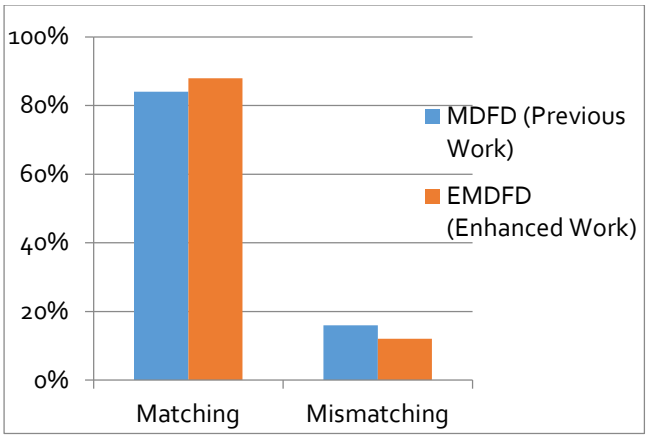

Figure 22: Similarity Results for MDFD and EMDFD

To test the robustness of our method, query images of real tumors were fed into the system using a similarity threshold value of 0.4 (minimum 60% match). As can be seen in Figure 23, the resulting images are satisfactorily similar to the query image. Because the retrieved images are invariant to rotation (1,2 and 3 of Figure 23) and scaling effects (5 of Figure 23), the method is suitable for real case mammogram ROI images.

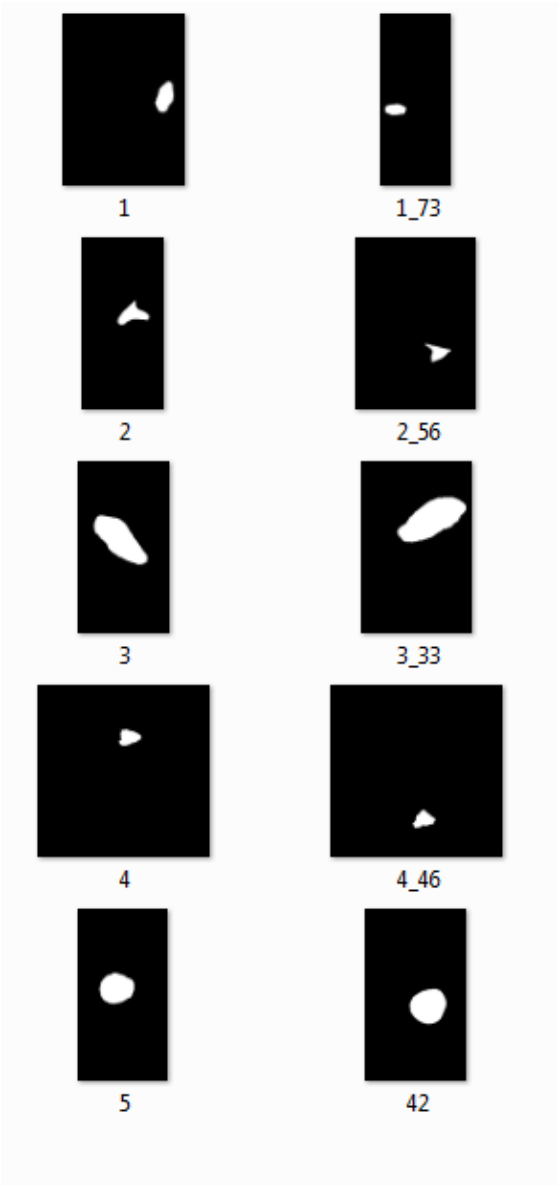

Figure 23: Similar Images Retrieved for Real Case Images When Exact Match is not Found in the Database

7. CONCLUSIONS

Results in Figures 17 and 18 show that MDFD provides greater similarity measurement than SOM. The proposed method (MDFD) also shows robustness to rotation, scaling and starting point of the images, which is an important aspect to be considered for the similarity measurement. Hence, this paper achieved its goal in finding a better method for extracting the most similar image from a database in order to provide better information to radiologists for early breast cancer diagnosis. Also, after testing with several types of images, it was concluded that adding the filters to MDFD improved the overall performance of the system. Taking the global features such as area ratio, convexity, eccentricity and solidity into consideration proved to be helpful. As mentioned in [41, 42, 43], global features contain important information about images and considering them alongside local features provides a better description of images, hence improving similarity measurement. Also, the method works well in similarity measurement for real cases images where exact similarity is difficult to find. The main objective of this paper to provide a better a more reliable way for similarity measurement of binary images as compared to MDFD which can help radiologists make better breast cancer diagnosis. Through the results, it is clear that EMDFD is superior to MDFD and the whole system is superior to SOM in similarity measurement.

As mentioned in [7,9], increased performance in similarity measurement of images increases as performance of CAD, thus improving the analysis of breast cancer. So, with the improved performance of the system, a useful contribution was made in the field of breast cancer analysis.

REFERENCES

1. Organization, W.H., 2014. World Cancer Report, 2014. *WHO Report. Geneva: WHO*
2. Society, A.C., 2015. *Cancer Facts & Figures 2015*. American Cancer Society.
3. Bozek, Jelena, Mario Mustra, Kresimir Delac, and Mislav Grgic. "A Survey of Image Processing Algorithms in Digital Mammography." In Recent Advances in Multimedia Signal Processing and Communications, pp. 631-657. Springer Berlin Heidelberg, 2009.
4. Qi, Hairong, and Wesley E. Snyder. "Content-Based Image Retrieval in Picture Archiving and Communications Systems." Journal of Digital Imaging 12.1 (1999): 81-83.
5. Wang, Zhiyong, Zheru Chi, and Dagan Feng. "Shape Based Leaf Image Retrieval." Vision, Image and Signal Processing, IEEE Proceedings-. Vol. 150. No. 1. IET, 2003.
6. Acha, B., Rangayyan, R.M., Desautels, J.E.L.: Detection of Microcalcifications in Mammograms. In: Suri, J.S., Rangayyan, R.M. (eds.) Recent Advances in Breast Imaging, Mammography, and Computer-Aided Diagnosis of Breast Cancer. SPIE, Bellingham (2006)
7. Nass, Sharyl J., I. Craig Henderson, and Joyce C. Lashof, eds. Mammography and Beyond: Developing Technologies for the Early Detection of Breast Cancer. National Academies Press, 2001.
8. Breast Cancer Imaging: A Multidisciplinary, Multimodality Approach By Marie Tartar, Christopher E. Comstock, Michael (2008)

9. H.D., Shi, X.J., Min, R., Hu, L.M., Cai, X.P., Du, H.N.: Approaches for Automated Detection and Classification of Masses in Mammograms. Pattern Recognition 39(4), 646–668 (2006)

10. Microwave Tomography: Review of the Progress Towards Clinical Applications

11. Wendie, A., M. D. Berg, and D. Jeffrey. "Combined Screening with Ultrasound and Mammography Compared to Mammography Alone in Women at Elevated Risk of Breast Cancer: Results of the First-Year Screen in ACRIN 6666." JAMA 299.18 (2008): 2151-2163.

12. Nayeem, Fatima, et al. "Similarity of Fibroglandular Breast Tissue Content Measured from Magnetic Resonance and Mammographic Images and by a Mathematical Algorithm." International Journal of Breast Cancer 2014 (2014).

13. Łuczyńska, Elżbieta, et al. "Comparison Between Breast MRI and Contrast-Enhanced Spectral Mammography." Medical Science Monitor: International Medical Journal of Experimental and Clinical Research 21 (2015): 1358.

14. Yang, Shih-Neng, et al. "Identification of Breast Cancer Using Integrated Information from MRI and Mammography." PloS one 10.6 (2015): e0128404.

15. Aminikhanghahi, Samaneh, et al. "Effective Tumor Feature Extraction for Smart Phone Based Microwave Tomography Breast Cancer Screening."Proceedings of the 29th Annual ACM Symposium on Applied Computing. ACM, 2014.

16. Celebi, M.E. and Aslandogan, Y.A., 2005. A Comparative Study of Three Moment-Based Shape Descriptors. In Information Technology: Coding and Computing, 2005. ITCC 2005. International Conference on IEEE, 788-793.

17. El-ghazal, A., Basir, O., and Belkasim, S., 2009. Farthest Point Distance: A New Shape Signature for Fourier Descriptors. Signal Processing: Image Communication 24, 7, 572-586.

18. El-Kwae, E.A., Xu, H., and Kabuka, M.R., 2000. Content-Based Retrieval in Picture Archiving and Communication Systems. J Digit Imaging 13, 2 (May), 70-81.

19. Mokhtarian, F. and Bober, M., 2011. Curvature Scale Space Representation: Theory, Applications, and MPEG-7 Standardization. Springer Publishing Company, Incorporated

20. Da Fontoura Costa, L. and Cesar Jr, R.M., 2010. Shape Analysis and Classification: Theory and Practice. CRC Press.

21. D. Mumford, Mathematical Theories of Shape: Do They Model Perception? In: SPIE Conference on Geometric Methods in Computer Vision. vol. 1570 San Diego, California, 1991, pp. 2–10.

22. I. Biederman, Recognition-by-Components: A Theory of Human Image Understanding, Psychological Review 94 (1987) 115–147.

23. M. Hu, Visual Pattern Recognition by Moment Invariants, IRE Transactions on Information Theory IT–8 (1962) 115–147.

24. J. Flusser, On the Independence of Rotation Moment Invariants, Pattern Recognition 33 (2000) 1405–1410.

25. M. Teague, Image Analysis Via the General Theory of Moments, Journal of the Optical Society of America 70 (1980) 920–930.

26. A. Khotanzad, Invariant Image Recognition by Zernike Moments, IEEE Transactions on Pattern Analysis and Machine Intelligence 12 (1990) 489–497.

27. T. Zahn, R.Z. Roskies, Fourier Descriptors for Plane Closed Curves, IEEE Transactions on Computers 21 (1972) 269–281.

28. T.P. Wallace, P.A. Wintz, An Efficient Three Dimensional Aircraft Recognition Algorithm Using Normalized Fourier Descriptors, Computer Graphics and Image Processing 13 (1980) 99–126.

29. I. Kunttu, L. Lepisto, J. Rauhamaa, A. Visa, Multiscale Fourier Descriptors for Defect Image Retrieval, Pattern Recognition Letters 27 (2006) 123–132.

30. F. Mokhtarian, A. Mackworth, Scale-Based Description and Recognition of Planar Curves and Two-Dimensional Shapes, IEEE Transactions on Pattern Analysis and Machine Intelligence 8 (1986) 34–43.

31. S. Abbasi, F. Mokhtarian, J. Kittler, Curvature Scale Space Image in Shape Similarity Retrieval, Multimedia Systems 7 (1999) 467–476.

32. S. Abbasi, F. Mokhtarian, J. Kittler, Enhancing CSS-Based Shape Retrieval for Objects with Shallow Concavities, Image and Vision Computing 18 (2000) 199–211.

33. G. Chauang, C. Kuo, Wavelet Descriptor of Planar Curves: Theory and Applications, IEEE Transactions on Image Processing 5 (1996) 56–70.

34. R.B. Yadav, N.K. Nishchal, A.K. Gupta, V.K. Rastogi, Retrieval and Classification of Shape-Based Objects Using Fourier, Generic Fourier, and Wavelet-Fourier Descriptors Technique: A Comparative Study, Optics and Lasers in Engineering 45 (2007) 695–708.

35. T. Adamek, N.E. O'Connor, A Multiscale Representation Method for Non-Rigid Shapes with a Single Closed Contour, IEEE Transactions on Circuits and Systems for Video Technology 14 (2004) 742–753.

36. S. Junding, W. Xiaosheng, Chain Code Distribution-Based Image Retrieval, in: International Conference on Intelligent Information Hiding and Multimedia Signal Processing China, 2006, pp. 139–142.

37. E. Attalla, P. Siy, Robust Shape Similarity Retrieval Based on Contour Segmentation Polygonal Multiresolution and Elastic Matching, Pattern Recognition 38 (2005) 2229–2241.

38. E. Persoon, K.S. Fu, Shape Discrimination Using Fourier Descriptors, IEEE Transactions on Pattern Analysis and Machine Intelligence 8 (1986) 388–397.

39. D.S. Zhang, G. Lu, A Comparative Study of Curvature Scale Space and Fourier Descriptors, Journal of Visual Communication and Image Representation 14 (2003) 41–60.

40. Zhang, D. and Lu, G., 2001. A Comparative Study on Shape Retrieval using Fourier Descriptors with Different Shape Signatures. In Proc. International Conference on Intelligent Multimedia and Distance Education (ICIMADE01).

41. Lisin, D., Mattar, M., Blaschko, M.B., Learned-Miller, E.G., and Benfield, M.C., 2005. Combining Local and Global Image Features for Object Class Recognition. In Computer Vision and Pattern Recognition-Workshops, 2005. CVPR Workshops. IEEE Computer Society Conference on IEEE, 47-47.

42. Eisa, M., 2014. Combined Local and Global Features for Improving the Shape Retrieval. *International Journal of Computer Science Issues (IJCSI) 11*, 3, 12.

43. Wu, Y. and Wu, Y., 2009. Shape-Based Image Retrieval Using Combining Global and Local Shape Features. In *Image and Signal Processing, 2009. CISP'09. 2nd International Congress on* IEEE, 1-5.

44. Image Feature Extraction Techniques and Their Applications for CBIR and Biometrics Systems

45. Advances in Computer Vision and Information Technology By K. V. Kale

46. A Review on Image Feature Extraction and Representation Techniques Dong ping Tian1,2

47. Yang, Mingqiang, Kidiyo Kpalma, and Joseph Ronsin. "A Survey of Shape Feature Extraction Techniques." Pattern recognition (2008): 43-90.

48. T. Pavlidis, Algorithms for Graphics and Image Processing, Computer Science Press, Rockville, MD, 1982, p. 143.

49. Bernier T., Landry J.A., ―A New Method for Representing and Matching Shapes of Natural Objects, ‖ Pattern Recognition, vol. 36, 2003, pp.1711 – 1723.

50. Kindratenko V.V., ―On Using Functions to Describe the Shape,‖ Journal of Mathematical Imaging and Vision, vol. 18, no. 3, 2003, pp.225 – 245.

51. Kunttu I., Lepistö L., Rauhamaa J. and Visa A., ―Multiscale Fourier Descriptor for Shape Classification,‖ Proceedings of the 12th International Conference on Image Analysis and Processing (ICIAP'03), 2003, pp.54-59.

52. Kunttu I., Lepistö L., Rauhamaa J., and Visa A., ―Multiscale Fourier Descriptor for Shape-Based Image Retrieval,‖ Proceedings of the 17th International Conference on Pattern Recognition (ICPR'04), 2004, pp.32-37.

53. Chalechale A., Mertins A., Naghdy G., ―Edge Image Description Using Angular Radial Partitioning, ‖ Vision Image and Signal Processing, vol. 151, no. 2, 2004, pp.93 – 101.

54. Zhang D., Lu G., ―Study and Evaluation of Different Fourier Methods for Image Retrieval, ‖ Image and Vision Computing, vol. 23, no. 11, 2005, pp.33-49.

55. G. Eichmann, C. Lu, M. Jankowski, R. Tolimieri, Shape Representation by Gabor Expansion, in: Hybrid Image and Signal Processing II. vol. 1297, 1990, pp. 86–94.

56.] K. Arbter, Affine-Invariant Fourier Descriptors, In: From Pixels to Feature, Elsevier Science, Amsterdam, The Netherlands, 1989.

57. [26] K. Arbter, W.E. Snyder, H. Burkhardt, G. Hirzinger, Application of Affine-Invariant Fourier Descriptors to Recognition of 3-D objects, IEEE Transactions

58. I. Bartolini, P. Ciaccia, M. Patella, WARP: Accurate Retrieval of Shapes Using Phase of Fourier Descriptors and Time Warping Distance, IEEE Transactions on Pattern Analysis and Machine Intelligence 27 (2005) 142–147.

59. Mocanu I., ―Image Retrieval by Shape Based on Contour Techniques - A Comparative Study, ‖ IEEE-4th International Symposium on Applied Computational Intelligence and Informatics, 2007, pp.34-39.

60. Guru D.S., Nagendraswamy H.S., ―Symbolic Representation of Two-Dimensional shapes,‖ Pattern Recognition Letters, 28, 2007, pp.144–155.

61. Conseil S., Bourennane S. and Martin L., ―Comparison of Fourier Descriptors and HU Moments for Hand Posture Recognition, ‖ 15th European Signal Processing Conferen ce (EUSIPCO 2007), Poznan, Poland, 2007, pp.1960-1964.

62. Zhang, Dengsheng, and Guojun Lu. "A Comparative Study on Shape Retrieval Using Fourier Descriptors with Different Shape Signatures." Proc. International Conference on Intelligent Multimedia and Distance Education (ICIMADE01). 2001.

63. A. K. Jain. Fundamentals of Digital Image Processing. Information and Systems Science Series. Prentice Hall, 1989.

64. B. J¨ahne. Digital Image Processing. Springer, Berlin, 4 edition, 1997.

65. Zhang, Dengsheng, and Guojun Lu. "A Comparison of Shape Retrieval Using Fourier Descriptors and Short-Time Fourier Descriptors." Advances in Multimedia Information Processing—PCM 2001. Springer Berlin Heidelberg, 2001. 855-860.

66. Quang Minh Tieng and W. W. Boles Recognition of 2-D Object Contours Using the Wavelet Transform Zero-Crossing Representation IEEE Trans. on PAMI 19(8) Aug.1997

67. Hee Soo Yang, Sang Uk Lee, Kyoung Mu Lee. Recognition of 2-D Object Contours Using Starting-Point-Independent Wavelet Coefficient Matching. Journal of Visual Communication and Image Representation, Vol. 9, No. 2, Jun 1998, pp. 171-181.

68. Jung, B.K., Wang, W., Li, Z., Son, S.H., and Kim, J.Y., 2012. A Sectorized Object Matching Approach for Breast Magnetic Resonance Image Similarity Study. In *Proceedings of the 2012 ACM Research in Applied Computation Symposium* ACM, 172-175.